

SUDO: Enhancing Text-to-Image Diffusion Models with Self-Supervised Direct Preference Optimization

Liang Peng^{1*†} Boxi Wu^{2*} Haoran Cheng^{2*} Yibo Zhao^{1,2} Xiaofei He^{1,2}

¹FABU Inc. ²Zhejiang University

{pengliang, wuboxi, chenghaoran}@zju.edu.cn

Abstract

Previous text-to-image diffusion models typically employ supervised fine-tuning (SFT) to enhance pre-trained base models. However, this approach primarily minimizes the loss of mean squared error (MSE) at the pixel level, neglecting the need for global optimization at the image level, which is crucial for achieving high perceptual quality and structural coherence. In this paper, we introduce Self-sUpervised Direct preference Optimization (SUDO), a novel paradigm that optimizes both fine-grained details at the pixel level and global image quality. By integrating direct preference optimization into the model, SUDO generates preference image pairs in a self-supervised manner, enabling the model to prioritize global-level learning while complementing the pixel-level MSE loss. As an effective alternative to supervised fine-tuning, SUDO can be seamlessly applied to any text-to-image diffusion model. Importantly, it eliminates the need for costly data collection and annotation efforts typically associated with traditional direct preference optimization methods. Through extensive experiments on widely-used models, including Stable Diffusion 1.5 and XL, we demonstrate that SUDO significantly enhances both global and local image quality. The codes are provided at [this link](#).

1. Introduction

The advancement of text-to-image diffusion models [11, 20, 27, 28, 32, 39] has sparked significant progress in generative AI, particularly in producing high-quality images from textual descriptions. These models are typically trained on large datasets and can be fine-tuned on a high-quality dataset using supervised fine-tuning (SFT) [5, 8]. SFT focuses on optimizing the model by minimizing the mean squared error (MSE) loss in the latent space, with the goal of refining the model’s noise predictions at the per-pixel

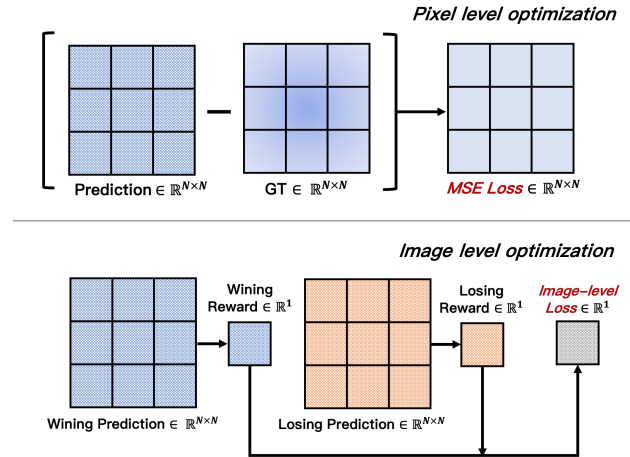


Figure 1. Pixel-level and image-level optimization. In the conventional fine-tuning process, previous diffusion methods typically focus on pixel-level MSE loss. We enhance text-to-image diffusion models by incorporating image-level learning, achieved through self-supervised direct preference optimization.

level. However, this fine-tuning process primarily addresses local discrepancies within the pixel, failing to account for the global optimization of the entire image. As a consequence, the model may struggle to generalize across diverse inputs, potentially leading to reduced image quality and poorer text-image alignment in generated outputs.

To mitigate these limitations, we propose Self-sUpervised Direct preference Optimization (SUDO), which incorporates global-level learning [31, 37] in a self-supervised manner. In contrast to SFT’s focus on fine-grained pixel-level predictions through MSE loss, SUDO jointly optimizes the model at the global image level using preference image pairs. We illustrate the core idea of image-level learning in Figure 1. Such image pairs are generated by downgrading image labels in a self-supervised fashion, *i.e.*, text-image perturbation. This strategy encourages the model to learn from both local and global contexts within the latent space, thereby capturing richer and more informative patterns. Unlike traditional direct preference optimization (DPO) methods [31, 37], which often rely on costly col-

*Equal contribution

†Work was done at FABU Inc.

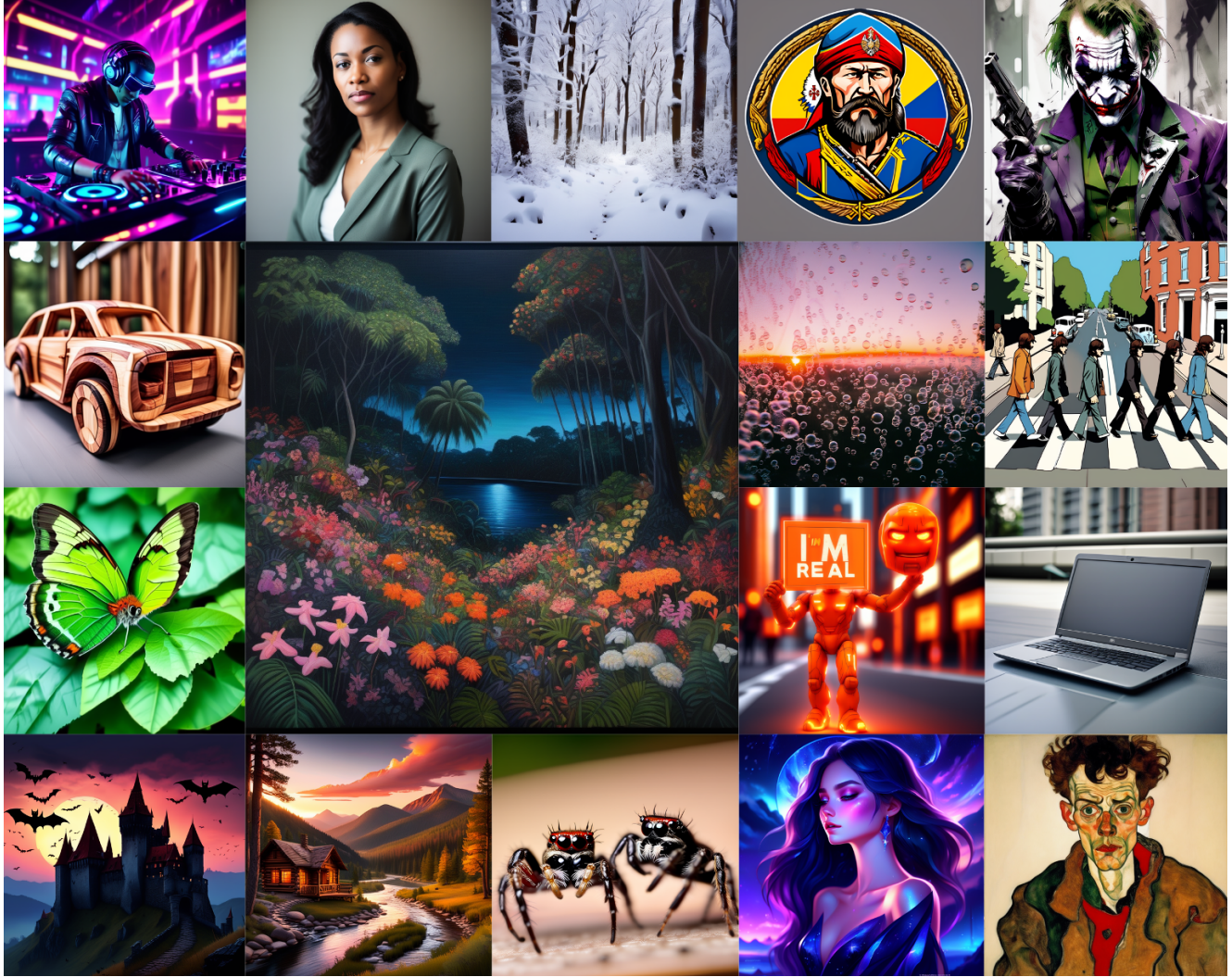


Figure 2. We develop SUDO, a method for fine-tuning text-to-image diffusion models. It incorporates direct preference optimization in a self-supervised manner. We provide the results generated by the fine-tuned SDXL model with our method. Best viewed in color.

Data requirements	SFT	SUDO	DPO
Text Prompt	✓	✓	✓
Image	✓	✓	✓
Preference Image	-	-	✓

Table 1. Data requirements for different fine-tuning manners. The proposed SUDO shares the same data requirements as SFT. DPO needs extra preference images that are collected and annotated by human, which is highly time-consuming and expensive.

lections and human annotations, SUDO’s self-supervised design eliminates the need for expensive labeled datasets. We summarize the training data requirements in Table 1.

Importantly, SUDO is model-agnostic and can be applied to most text-to-image diffusion models. It offers an alternative to SFT, providing performance gains without extra manual annotations or dataset modifications. Our experiments on popular models such as Stable Diffusion 1.5 [32]

and XL [28] show that SUDO yields substantial improvements in both overall image quality and text-image alignment. Furthermore, when compared to DPO approaches [37], SUDO demonstrates significant enhancements despite using only self-supervised preference images rather than manually annotated pairs, underscoring its potential to advance text-to-image diffusion models. As shown in Figure 2, we provide some visualization results using the fine-tuned SDXL model with SUDO.

In summary, we introduce SUDO as a self-supervised method to direct preference optimization, consistently enhancing model performance in text-to-image generation tasks. This manner opens promising avenues for future work and underscores the value of global-level learning.

2. Related Work

2.1. Text-to-Image Diffusion Models

Text-to-image diffusion models have recently attracted significant attention in generative modeling due to their ability to produce high-quality and diverse images from textual descriptions. The introduction of Denoising Diffusion Probabilistic Models (DDPMs) [9, 17] marked a major breakthrough in this field, establishing diffusion models as a powerful generative approach. These models operate by reversing a gradual diffusion process, where noise is incrementally added to an image and then learned to be removed, ultimately synthesizing a coherent and realistic image. Building upon this foundation, diffusion models have become a representative paradigm in text-to-image generation, leading to models like GLIDE [25] for text-guided image editing, Imagen [33] with cascaded diffusion for high-resolution synthesis, and Stable Diffusion [32] using latent diffusion for efficient generation. To enhance image generation quality, researchers typically focus on two main directions. One approach involves architectural improvements, with the Diffusion Transformer (DiT) [27] gaining attention for its improved image fidelity, performance, and diversity. Notable advancements include PixArt- α [5], Hunyuan-DiT [23], and SD3 [11]. Another approach leverages supervised fine-tuning to refine text-to-image diffusion models. These methods curate datasets by integrating various strategies, such as preference models [28], pre-trained image models [2, 10, 38] (e.g., image captioning models), and expert-assisted data filtering [8].

2.2. Preference-Based Optimization Methods

In recent years, preference-based optimization has gained traction, refining models through user feedback or ranked preference pairs. In Large Language Models, Reinforcement Learning from Human Feedback (RLHF) leverages human comparisons to train a reward model that guides policy learning [1, 26]. Alternatively, direct preference optimization (DPO) fine-tunes models directly on preference data, bypassing the need for an explicit reward model while achieving comparable performance [31]. Subsequently, preference-based optimization has been applied to image generation. Some methods enhance image quality by increasing rewards for preferred outputs [7, 14, 29], while others use reinforcement learning [3, 14]. However, training reliable reward models remains challenging and computationally expensive, with over-optimization potentially leading to mode collapse, reducing diversity [21, 29]. Similarly, Direct Preference Optimization has been introduced in text-to-image generation, with Diffusion-DPO [37] demonstrating the effectiveness of optimizing on human comparison data to enhance both visual appeal and text alignment. Additionally, direct score preference optimization [44] re-

finer diffusion models through score matching, providing a novel approach to preference learning. Several recent studies have further explored adapting preference learning techniques from large language models to fine-tune diffusion models [22, 41, 43], highlighting the growing interest in aligning generative models with human preferences.

2.3. Self-Supervised Learning

Self-supervised learning has emerged as a pivotal paradigm in machine learning. Among its most widely used approaches are contrastive self-supervised learning and generative self-supervised learning. Contrastive self-supervised learning distinguishes representations by pulling similar instances closer while pushing dissimilar ones apart. MoCo [15] enhances training efficiency through a momentum encoder, while SimCLR [6] simplifies the process with strong data augmentations. CLIP [30] extends contrastive learning to vision-language tasks, aligning images and text in a shared latent space, enabling zero-shot transfer. Generative approaches inherently follow unsupervised or self-supervised learning principles, training without labeled data to model the underlying distributions of the input. GANs [13] utilize adversarial training to generate realistic data, while VAEs [18] encode data into a structured latent space for controlled synthesis. VQ-VAE [36] introduces discrete latent representations for high-quality generation. MAE [16] leverages masked image modeling to learn rich visual features. More recently, denoising diffusion models [17] have demonstrated impressive results by iteratively adding and removing noise, learning robust representations in a self-supervised manner. Self-supervised learning enables training without manually labeled data, laying the foundation for future advancements in representation learning, generative modeling, and multimodal understanding.

3. Methods

3.1. Preliminary

Diffusion Models. Denoising Diffusion Probabilistic Models [17] represent the image generation process as a Markovian process. Let $\mathbf{x}_0 \in \mathbb{R}^d$ be the data point and $q(\mathbf{x}_t|\mathbf{x}_{t-1})$ denote the forward process, where noise is added to the data at each timestep t . The forward process is defined as:

$$q(\mathbf{x}_t|\mathbf{x}_{t-1}) = \mathcal{N}(\mathbf{x}_t; \sqrt{1 - \beta_t}\mathbf{x}_{t-1}, \beta_t\mathbb{I}), \quad (1)$$

where β_t is a schedule that controls the variance of noise added at each timestep, and $\mathcal{N}(\cdot)$ denotes the normal distribution. The forward process gradually adds noise, with \mathbf{x}_T being pure noise after T timesteps. The reverse process aims to learn the distribution $p_\theta(\mathbf{x}_{t-1}|\mathbf{x}_t)$, which represents the process of denoising and generating data from pure noise. The reverse process can be parameterized as:

$$p_\theta(\mathbf{x}_{t-1}|\mathbf{x}_t) = \mathcal{N}(\mathbf{x}_{t-1}; \mu_\theta(\mathbf{x}_t, t), \Sigma_\theta(\mathbf{x}_t, t)), \quad (2)$$

where $\mu_\theta(\mathbf{x}_t, t)$ and $\Sigma_\theta(\mathbf{x}_t, t)$ are the mean and covariance learned by the model at each timestep t . The model is trained by minimizing the following objective:

$$\mathcal{L}_{\text{diffusion}} = \mathbb{E}_{t, \mathbf{x}_0, \epsilon} [\|\epsilon - \epsilon_\theta(\mathbf{x}_t, t)\|^2], \quad (3)$$

where ϵ is the noise added at each timestep, and $\epsilon_\theta(\mathbf{x}_t, t)$ is the model’s predicted noise. The model is trained to predict this noise accurately at each step, enabling it to reverse the diffusion process and generate high-quality data.

Reinforcement Learning from Human Feedback. For diffusion models, human preferences at each diffusion step are modeled using a Bradley-Terry formulation [4], where the probability of preferring a “winning” sample \mathbf{x}_t^w over a “losing” sample \mathbf{x}_t^l for a given prompt \mathbf{c} is defined as:

$$p_{\text{BT}}(\mathbf{x}_t^w \succ \mathbf{x}_t^l | \mathbf{c}) = \sigma(r(\mathbf{c}, \mathbf{x}_t^w) - r(\mathbf{c}, \mathbf{x}_t^l)), \quad (4)$$

with σ, r, \mathbf{c} representing the sigmoid function, reward model, and prompt, respectively. Subsequently, by conceptualizing the diffusion denoising process as a multi-step Markov Decision Process, the generative model is fine-tuned via reinforcement learning. The training objective [12, 37] is formulated as:

$$\mathcal{L}_{\text{rlhf}} = \mathbb{E}_{\mathbf{c} \sim D} \mathbb{E}_{p_\theta(\mathbf{x}_{0:T} | \mathbf{c})} \sum_{t=0}^{T-1} r(\mathbf{c}, \mathbf{x}_t) - \lambda \mathbb{D}_{\text{KL}}(p_\theta(\mathbf{x}_{0:T} | \mathbf{c}) \| p_{\text{ref}}(\mathbf{x}_{0:T} | \mathbf{c})), \quad (5)$$

where $p_{\text{ref}}(\mathbf{x}_{0:T} | \mathbf{c})$ is the distribution from the pretrained diffusion model and λ controls the influence of the KL divergence regularization term.

Direct Preference Optimization (DPO). DPO streamlines RLHF by using the learning policy’s log likelihood to implicitly encode the reward. In text-to-image diffusion models, this leads to a step-wise reward defined as:

$$r(\mathbf{c}, \mathbf{x}_t) = \lambda \log \frac{p_\theta(\mathbf{x}_t | \mathbf{x}_{t+1}, \mathbf{c})}{p_{\text{ref}}(\mathbf{x}_t | \mathbf{x}_{t+1}, \mathbf{c})}. \quad (6)$$

Recent works [37, 44] follow this line and adapt it to diffusion models. They optimize the model p_θ based on the Bradley-Terry model [4], leading to an objective function:

$$\mathcal{L}_{\text{Diffusion-DPO}} = -\mathbb{E} \left[\log \sigma \left(\lambda \log \frac{p_\theta(\mathbf{x}_t^w | \mathbf{x}_{t+1}^w, \mathbf{c})}{p_{\text{ref}}(\mathbf{x}_t^w | \mathbf{x}_{t+1}^w, \mathbf{c})} - \lambda \log \frac{p_\theta(\mathbf{x}_t^l | \mathbf{x}_{t+1}^l, \mathbf{c})}{p_{\text{ref}}(\mathbf{x}_t^l | \mathbf{x}_{t+1}^l, \mathbf{c})} \right) \right], \quad (7)$$

where the winning and losing samples $(\mathbf{x}_t^w, \mathbf{x}_t^l)$ and the prompt \mathbf{c} are drawn from the dataset, and timestep t is uniformly sampled from the diffusion process. This formulation effectively aligns the learning policy with human preference signals embedded in the reference model.

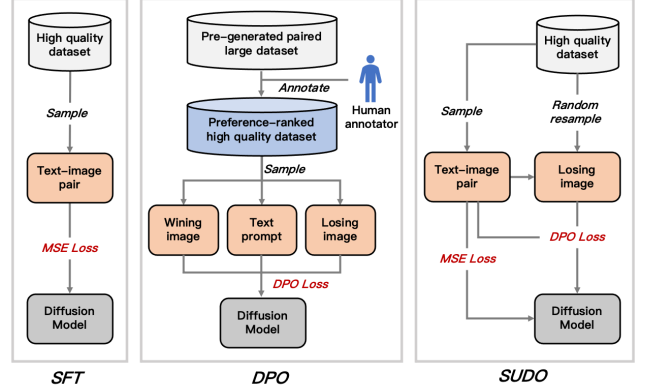


Figure 3. Different training process of SFT, DPO, and SUDO. We generate losing images in a self-supervised manner, to perform direct preference optimization under a regular dataset. Best viewed in color with zoom in.

3.2. SUDO for Text-to-image Diffusion Models

Inspired by DPO’s effective alignment with human preferences at the image level [37], our work aims to extend this formulation into the standard fine-tuning process for diffusion models. Unfortunately, a direct application of DPO is not feasible because it requires collecting image pairs (typically generated by different models with the same prompt or by using different seeds with the same model—along with their associated manual rankings). This approach does not align with the conventional fine-tuning pipeline and incurs significant additional costs. To overcome this limitation, we propose SUDO, which generates preference image pairs in a self-supervised manner.

In each training iteration, we denote the text-image pair as (\mathbf{c}, \mathbf{x}) , where the image component is regarded as the winning image \mathbf{x}^w . Traditional DPO methods [31, 37] require generating image pairs corresponding to the same prompt, followed by manual selection of the preferred (winning) and less preferred (losing) images, denoted as \mathbf{x}^w and \mathbf{x}^l , respectively. In contrast, our method eliminates the need for a manually selected the losing images. Instead, we obtain “self-generated losing samples” by systematically degrading the winner \mathbf{x}^w . Formally, the losing image is represented as $\mathbf{x}^{sl} = \text{Downgrade}(\mathbf{x}^w)$. Inspired by [37], the self-supervised direct preference loss is:

$$\mathcal{L}_{\text{SUDO}} = -\log \sigma \left(C \left[\|\epsilon_\theta(\mathbf{x}_t^w, t) - \epsilon^w\|_2^2 - \|\epsilon_\theta(\mathbf{x}_t^{sl}, t) - \epsilon^{sl}\|_2^2 - (\|\epsilon_{\text{ref}}(\mathbf{x}_t^w, t) - \epsilon^w\|_2^2 - \|\epsilon_{\text{ref}}(\mathbf{x}_t^{sl}, t) - \epsilon^{sl}\|_2^2) \right] \right), \quad (8)$$

where $\mathbf{x}^{sl} = \text{Downgrade}(\mathbf{x}^w)$

where C and ϵ^{sl} refer to a scale factor and the noise corresponding to losing images, and ϵ_{ref} is the reference model. In our implementation, the **Downgrade** operation is sim-

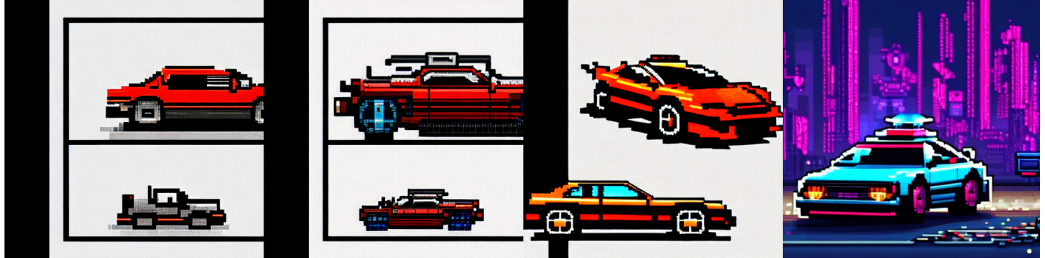
Andrew Huang riding a pink fluffy unicorn



hdr 8k resolution highly detailed image of a fairy by artist "Jasmine Becket Griffith" + Brian Froud



pixelart of a cyberpunk car



Tall fat man white background t-shirts



A Great dane dog in the style of Vincent Van Gogh



SD1.5

DPO

SFT

SUDO

Figure 4. Qualitative comparisons with the SD1.5 base model. All results are generated with the same random seed. Comparing with SFT and DPO [37], the model trained by SUDO demonstrates superior text prompt alignment. It also shows more appealing visual quality, especially in layout, colors, and details. Best viewed in color.

ply performed by randomly selecting images from the training dataset. Namely, for each self-generated image pair, the winning sample closely aligns with the prompt, whereas the losing sample fails to correspond to the description. We encourage future work to explore more degradation strategies for self-supervised direct preference optimization. The training process overview is shown in Figure 3. s

Overall Loss. Concerning the above discussion, the final loss is as follows:

$$\mathcal{L} = \lambda_1 \mathcal{L}_{\text{MSE}} + \lambda_2 \mathcal{L}_{\text{SUDO}} \quad (9)$$

We empirically set λ_1 and λ_2 to 0.5, 0.5, respectively. \mathcal{L}_{MSE} makes the model focus on pixel level optimization, and $\mathcal{L}_{\text{SUDO}}$ encourages the model to learn information on the image level. Such two losses are complementary.

4. Experiments

4.1. Setup

Implement Details: Following Diffusion-DPO [37], for the SD1.5 [32] experiments, AdamW [24] is utilized, while SDXL [28] training is conducted with Adafactor [35] to conserve memory. Following the official implementation in Diffusion-DPO [37], C in Equation 8 is set to -2500 . For SD 1.5, a batch size of 2048 pairs (resolution: $512 * 512$) is maintained by training across 4 NVIDIA A100 GPU. Each handling 8 pairs locally with gradient accumulation over 64 steps. For SDXL, considering the resource limitation, we use the total batch size of 96 pairs (resolution: $1024 * 1024$). Training is performed at fixed square resolutions. We use a learning rate of $1e-6$ coupled with a 25% linear warmup.

Training Dataset: Our training data is sourced from the Pick-a-Pic V2 dataset[19], which keeps the same to Diffusion-DPO [37]. It contains pairwise preference annotations for images generated by Dreamlike (a fine-tuned variant of SD1.5), SD2.1, and SDXL. These prompts and preferences were collected from users of the Pick-a-Pic web application. *Please note that SUDO only uses the preference image and associated text in the dataset, instead of using the whole manually annotated image pairs.*

Evaluation: We conduct evaluation on three datasets: Pick-a-Pic V2 [19] validation set (contains 500 prompts), PartiPrompts [42] (contains 1632 prompts, including diverse categories and challenge aspects), and HPDV2 [38] (contains 3200 prompts, including anime, concept art, paintings and photo). We compare SUDO with three different type baselines, *i.e.*, base models (Stable Diffusion 1.5 (SD1.5) and Stable Diffusion XL (SDXL)), SFT models, DPO models, where DPO models are the publicly released from Diffusion-DPO [37]. For evaluation metrics, we employ the popular PickScore [19], Aesthetics [34], CLIP [30], HPS V2 [38], and ImageAward [40] scores. For convenience of comparison, we scale the scores to fit a similar range ($\times 100$ for PickScore, CLIP, HPS, and ImageAward, $\times 10$ for Aesthetics). **PickScore** is a caption-sensitive scoring model, originally trained on Pick-a-Pic (v1), that estimates the perceived image quality by humans. **Aesthetics** assesses the visual appeal of an image, considering factors such as lighting, color harmony, composition, and overall artistic quality. **CLIP** measures the semantic alignment between an image and a corresponding text prompt. By computing the cosine similarity between the image and text embeddings, this score evaluates how well the image content matches the provided textual description. **Human Preference Score (HPS V2)** is a metric designed to align with human judgments of image quality, particularly in the context of text-to-image synthesis. **ImageAward** quantifies the

quality, aesthetic appeal, or alignment of a generated image with respect to desired attributes. It is typically derived from a reward model trained on human preference data.

4.2. Quantitative Results

s We provide quantitative comparisons in Table 2. We compare our method with SFT and DPO [37]. For the SD1.5 base model, our method significantly outperforms the alternatives. For example, SUDO achieves a CLIP score of 34.79 on the Pick-a-Pic V2 dataset—an improvement of +2.21 over the base model—whereas SFT and DPO yield improvements of +1.17 and +0.61, respectively. In terms of overall human preference metrics, SUDO delivers substantially higher gains, improving the base model from -14.81 to 71.00 on the ImageReward metric, which far exceeds the improvements observed with SFT (45.03) and DPO (4.13). Notably, the win rate of SUDO reaches 94.20 on the HPS metric. Results on other datasets (PartiPrompts and HPD v2) further confirm these improvements. In contrast, results on the SDXL base model show a slightly different scenario, particularly with SFT. We observe that SFT substantially degrades the performance of the base model. This degradation is likely due to the fact that, while the training dataset (comprising generations from an SD1.5 variant, SD2.1, and SDXL) is of much higher quality than that used for SD1.5, it does not exhibit clear superiority for SDXL. Nevertheless, the model trained by SUDO still demonstrates significantly better performance compared to both SFT and the base model. On the PickScore, Aesthetics, and CLIP metrics, SUDO achieves results comparable to DPO, and it attains superior scores on the HPS and ImageReward metrics. These findings validate our hypothesis that image-level learning benefits text-to-image diffusion models and highlight the superiority of SUDO.

4.3. Qualitative Results

We provide qualitative comparisons in Figure 4 and Figure 1 for SD1.5 and SDXL, respectively. All quantitative and qualitative results are generated using the same random seed. We observe that SUDO consistently improves over other models, particularly in terms of producing more vivid colors and better adherence to text prompts. For example, in the third row of Figure 4, only SUDO successfully reveals the concept "cyberpunk". In the fourth row of Figure 1, both DPO and SUDO capture the intended meaning of the prompt, but SUDO exhibits a more appealing visual quality. These quantitative and qualitative results confirm the effectiveness of our approach.

4.4. Ablation

We conduct ablation studies on various downgrade approaches, as shown in Table 3. In particular, we examine two additional methods—namely, blur (which involves

Prints, Ink, Paper, Relief prints, Woodblock prints, Printing blocks, Wood blocks, Asia, Japan, ca. 1853, Japan, Polychrome woodblock print; ink and color on paper, Metropolitan Museum of Art



Harry potter as a cat, pixar style, octane render, HD, high-detail



Cadillao El Dorado de style Badass Steampunk dans une vieille rue pavée, trending on artstation, sharp focus, studio photo, intricate details, highly detailed, by greg rutkowski



a marine iguana on a surfboard



character sheet, The little girl riding an electric scooter bike, in a beautiful anime scene by Hayao Miyazaki: a snowy Tokyo city with massive Miyazaki clouds floating in the blue sky, enchanting snowscapes of the city with bright sunlight, Miyazaki's landscape imagery, Japanese art, 16:9



SDXL

DPO

SFT

SUDO

Figure 5. Qualitative comparisons with the SDXL base model. All results are generated using the same random seed. Please note that the training dataset (Pick-a-Pic V2 [19]) used for fine-tuning is obtained from a SD1.5 variant, SD2.1, and SDXL models. Consequently, directly fine-tuning (SFT) on this dataset does not lead to improvements—and may even result in degraded performance (e.g., as shown in the second row). In contrast, DPO [37] optimizes the model by leveraging preference relationships with pre-ranked pairs, thereby avoiding this issue. SUDO uses the same data requirements as SFT but yields significant improvements in both text prompt alignment and visual quality, demonstrating its effectiveness. Best viewed in color.

downsampling and upsampling the image by a factor of 4) and random grid (which divides the image into an 8×8 grid and randomly swaps two grids). We observe that these two downgrade methods lead to worse performance than SFT, indicating that significantly degraded image quality is harm-

ful for image-level preference learning. Additionally, we remove the MSE loss and report the results in Table 4. Interestingly, the performance does not drop noticeably, further confirming the effectiveness of image-level learning and the SUDO approach.

Datasets	Methods		SD1.5					SDXL				
			P.S.	Aes.	CLIP	HPS	I.R.	P.S.	Aes.	CLIP	HPS	I.R.
Pick-a-Pic V2	Base	Avg score	20.57	53.15	32.58	26.17	-14.81	22.10	60.01	35.86	26.83	50.62
	SFT		21.10	56.35	33.75	27.03	45.03	21.48	57.84	35.67	26.67	30.89
	DPO		20.91	54.07	33.19	26.46	4.13	22.57	59.93	37.30	27.30	81.14
	SUDO		21.23	56.35	34.79	27.33	71.00	22.34	59.97	37.53	27.89	103.96
	SFT	Win rate	75.00	77.20	60.40	90.20	80.00	19.40	31.80	47.00	44.60	42.4
	DPO		73.80	60.00	60.00	71.80	61.00	72.60	47.20	63.00	79.80	69.8
SUDO	78.60		77.80	68.40	94.20	85.20	60.80	50.80	62.40	93.80	79.2	
PartiPrompts	Base	Avg score	21.39	53.13	33.21	26.79	1.48	22.63	57.69	35.77	27.33	69.78
	SFT		21.75	55.31	33.93	27.57	50.75	22.02	56.41	35.31	27.13	47.29
	DPO		21.61	53.58	33.88	26.98	21.43	22.90	57.85	36.95	27.73	103.36
	SUDO		21.84	55.09	35.11	27.84	75.66	22.79	58.69	37.00	28.30	117.50
	SFT	Win rate	67.28	70.89	53.43	85.42	73.35	21.38	38.11	45.10	43.75	40.93
	DPO		67.10	57.17	56.74	61.83	63.05	63.42	53.62	62.32	73.10	68.44
SUDO	69.85		68.50	63.24	89.40	81.00	56.19	60.48	60.17	92.16	76.84	
HPD V2	Base	Avg score	20.84	54.32	33.96	26.84	-11.79	22.78	61.34	37.68	27.68	78.27
	SFT		21.57	57.41	35.26	27.89	57.74	22.24	60.08	37.39	27.76	66.62
	DPO		21.30	55.80	34.68	27.22	13.24	23.18	61.35	38.45	28.14	102.74
	SUDO		21.58	57.10	36.30	28.11	76.13	22.98	61.30	38.35	28.77	110.67
	SFT	Win rate	79.53	75.31	59.34	90.10	81.16	23.47	37.28	46.63	58.22	45.81
	DPO		75.72	66.28	57.56	72.43	64.69	72.66	50.28	58.69	80.56	69.78
SUDO	79.53		74.03	68.47	92.49	85.19	58.78	48.06	55.65	94.97	72.50	

Table 2. Quantitative comparisons. We compare different fine-tuning methods (SFT, DPO [37], and SUDO) on SD 1.5 and SDXL base models over three datasets (Pick-a-Pic V2 [19], PartiPrompts [42], and HPDv2 [38]). "P.S." refers to PickScore, "Aes." is Aesthetics, and "I.R." denotes ImageAward.s For the SD1.5 base model, our method achieves the best performance across most metrics. In contrast, for the SDXL base model, we observe that SFT clearly degrades performance. This is likely due to the fact that the training dataset (Pick-a-pic V2 [19]) used for fine-tuning is derived from SD1.5 variant, SD2.1, and SDXL models. Interestingly, our method still achieves competitive results compared to DPO, which utilizes the full dataset and optimizes the model by leveraging preference relationships with pre-ranked pairs. These results underscore the effectiveness and robustness of our approach.

Methods	P.S.	Aes.	CLIP	HPS	I.R.
Base model	20.57	53.15	32.58	26.17	-14.81
SFT	21.10	56.35	33.75	27.03	45.03
w/ Blur	20.80	55.16	33.22	26.57	4.26
w/ Random grid	20.85	55.86	32.71	26.64	24.21
w/ Random image	21.23	56.35	34.79	27.33	71.00

Table 3. Ablation on different downgrade manners. Only the "Random image" row achieves significant improvements over SFT, implying that degrading the image quality is detrimental.

5. Limitation and Future Work

Our image-level learning is conducted using direct preference learning, which incurs additional computational cost during training—specifically, two forward passes (one for the winning image and one for the losing image) are required in each iteration. Furthermore, we currently downgrade the winning image by randomly selecting images

Methods	P.S.	Aes.	CLIP	HPS	I.R.
Base model	20.57	53.15	32.58	26.17	-14.81
SFT	21.10	56.35	33.75	27.03	45.03
SUDO w/o MSE	21.26	56.22	35.00	27.31	67.78
SUDO	21.23	56.35	34.79	27.33	71.00

Table 4. Ablation on MSE loss. When removing MSE loss, SUDO still shows the superiority to SFT.

from the training dataset. However, when the training dataset is very small, this strategy may prove ineffective. We encourage future work to explore more effective self-supervised methods for generating losing images.

6. Conclusion

In this paper, we propose incorporating image-level learning into the fine-tuning process for text-to-image diffusion tasks, which emphasizes global optimization. To address

this challenge, we introduce SUDO, a self-supervised approach based on direct preference optimization. In each training iteration, SUDO generates preference image pairs in a self-supervised manner and subsequently performs image-level learning. We conduct experiments on various datasets using different base models, demonstrating the effectiveness of the proposed method.

References

- [1] Yuntao Bai, Saurav Kadavath, Sandipan Kundu, Amanda Askell, Jackson Kernion, Andy Jones, Anna Chen, Anna Goldie, Azalia Mirhoseini, Cameron McKinnon, et al. Constitutional ai: Harmlessness from ai feedback. *arXiv preprint arXiv:2212.08073*, 2022. 3
- [2] James Betker, Gabriel Goh, Li Jing, Tim Brooks, Jianfeng Wang, Linjie Li, Long Ouyang, Juntang Zhuang, Joyce Lee, Yufei Guo, et al. Improving image generation with better captions. *Computer Science*. <https://cdn.openai.com/papers/dall-e-3.pdf>, 2(3):8, 2023. 3
- [3] Kevin Black, Michael Janner, Yilun Du, Ilya Kostrikov, and Sergey Levine. Training diffusion models with reinforcement learning. *arXiv preprint arXiv:2305.13301*, 2023. 3
- [4] Ralph Allan Bradley and Milton E Terry. Rank analysis of incomplete block designs: I. the method of paired comparisons. *Biometrika*, 39(3/4):324–345, 1952. 4
- [5] Junsong Chen, Jincheng Yu, Chongjian Ge, Lewei Yao, Enze Xie, Yue Wu, Zhongdao Wang, James Kwok, Ping Luo, Huchuan Lu, et al. Pixart- α : Fast training of diffusion transformer for photorealistic text-to-image synthesis. *arXiv preprint arXiv:2310.00426*, 2023. 1, 3
- [6] Ting Chen, Simon Kornblith, Mohammad Norouzi, and Geoffrey Hinton. A simple framework for contrastive learning of visual representations. In *International conference on machine learning*, pages 1597–1607. Pmlr, 2020. 3
- [7] Kevin Clark, Paul Vicol, Kevin Swersky, and David J Fleet. Directly fine-tuning diffusion models on differentiable rewards. *arXiv preprint arXiv:2309.17400*, 2023. 3
- [8] Xiaoliang Dai, Ji Hou, Chih-Yao Ma, Sam Tsai, Jialiang Wang, Rui Wang, Peizhao Zhang, Simon Vandenhende, Xi-aofang Wang, Abhimanyu Dubey, et al. Emu: Enhancing image generation models using photogenic needles in a haystack. *arXiv preprint arXiv:2309.15807*, 2023. 1, 3
- [9] Prafulla Dhariwal and Alexander Nichol. Diffusion models beat gans on image synthesis. *Advances in neural information processing systems*, 34:8780–8794, 2021. 3
- [10] Hanze Dong, Wei Xiong, Deepanshu Goyal, Yihan Zhang, Winnie Chow, Rui Pan, Shizhe Diao, Jipeng Zhang, Kashun Shum, and Tong Zhang. Raft: Reward ranked finetuning for generative foundation model alignment. *arXiv preprint arXiv:2304.06767*, 2023. 3
- [11] Patrick Esser, Sumith Kulal, Andreas Blattmann, Rahim Entezari, Jonas Müller, Harry Saini, Yam Levi, Dominik Lorenz, Axel Sauer, Frederic Boesel, et al. Scaling rectified flow transformers for high-resolution image synthesis. In *Forty-first international conference on machine learning*, 2024. 1, 3
- [12] Ying Fan, Olivia Watkins, Yuqing Du, Hao Liu, Moonkyung Ryu, Craig Boutilier, Pieter Abbeel, Mohammad Ghavamzadeh, Kangwook Lee, and Kimin Lee. Reinforcement learning for fine-tuning text-to-image diffusion models. In *Thirty-seventh Conference on Neural Information Processing Systems (NeurIPS) 2023*. Neural Information Processing Systems Foundation, 2023. 4
- [13] Ian Goodfellow, Jean Pouget-Abadie, Mehdi Mirza, Bing Xu, David Warde-Farley, Sherjil Ozair, Aaron Courville, and Yoshua Bengio. Generative adversarial nets. *Advances in neural information processing systems*, 27, 2014. 3
- [14] Yaru Hao, Zewen Chi, Li Dong, and Furu Wei. Optimizing prompts for text-to-image generation. *Advances in Neural Information Processing Systems*, 36:66923–66939, 2023. 3
- [15] Kaiming He, Haoqi Fan, Yuxin Wu, Saining Xie, and Ross Girshick. Momentum contrast for unsupervised visual representation learning. In *Proceedings of the IEEE/CVF conference on computer vision and pattern recognition*, pages 9729–9738, 2020. 3
- [16] Kaiming He, Xinlei Chen, Saining Xie, Yanghao Li, Piotr Dollár, and Ross Girshick. Masked autoencoders are scalable vision learners. In *Proceedings of the IEEE/CVF conference on computer vision and pattern recognition*, pages 16000–16009, 2022. 3
- [17] Jonathan Ho, Ajay Jain, and Pieter Abbeel. Denoising diffusion probabilistic models. *Advances in neural information processing systems*, 33:6840–6851, 2020. 3
- [18] Diederik P Kingma, Max Welling, et al. Auto-encoding variational bayes, 2013. 3
- [19] Yuval Kirstain, Adam Polyak, Uriel Singer, Shahbuland Matiana, Joe Penna, and Omer Levy. Pick-a-pic: An open dataset of user preferences for text-to-image generation. *Advances in Neural Information Processing Systems*, 36:36652–36663, 2023. 6, 7, 8
- [20] Black Forest Labs. Flux, 2024. Black Forest Labs. Flux, 2024. 1
- [21] Kimin Lee, Hao Liu, Moonkyung Ryu, Olivia Watkins, Yuqing Du, Craig Boutilier, Pieter Abbeel, Mohammad Ghavamzadeh, and Shixiang Shane Gu. Aligning text-to-image models using human feedback. *arXiv preprint arXiv:2302.12192*, 2023. 3
- [22] Shufan Li, Konstantinos Kallidromitis, Akash Gokul, Yusuke Kato, and Kazuki Kozuka. Aligning diffusion models by optimizing human utility. *Advances in Neural Information Processing Systems*, 37:24897–24925, 2025. 3
- [23] Zhimin Li, Jianwei Zhang, Qin Lin, Jiangfeng Xiong, Yanxin Long, Xincheng Deng, Yingfang Zhang, Xingchao Liu, Minbin Huang, Zedong Xiao, et al. Hunyuan-dit: A powerful multi-resolution diffusion transformer with fine-grained chinese understanding. *arXiv preprint arXiv:2405.08748*, 2024. 3
- [24] Ilya Loshchilov and Frank Hutter. Decoupled weight decay regularization. *arXiv preprint arXiv:1711.05101*, 2017. 6
- [25] Alex Nichol, Prafulla Dhariwal, Aditya Ramesh, Pranav Shyam, Pamela Mishkin, Bob McGrew, Ilya Sutskever, and Mark Chen. Glide: Towards photorealistic image generation and editing with text-guided diffusion models. *arXiv preprint arXiv:2112.10741*, 2021. 3

- [26] Long Ouyang, Jeffrey Wu, Xu Jiang, Diogo Almeida, Carroll Wainwright, Pamela Mishkin, Chong Zhang, Sandhini Agarwal, Katarina Slama, Alex Ray, et al. Training language models to follow instructions with human feedback. *Advances in neural information processing systems*, 35:27730–27744, 2022. 3
- [27] William Peebles and Saining Xie. Scalable diffusion models with transformers. In *Proceedings of the IEEE/CVF international conference on computer vision*, pages 4195–4205, 2023. 1, 3
- [28] Dustin Podell, Zion English, Kyle Lacey, Andreas Blattmann, Tim Dockhorn, Jonas Müller, Joe Penna, and Robin Rombach. Sdxl: Improving latent diffusion models for high-resolution image synthesis. *arXiv preprint arXiv:2307.01952*, 2023. 1, 2, 3, 6
- [29] Mihir Prabhudesai, Anirudh Goyal, Deepak Pathak, and Katerina Fragkiadaki. Aligning text-to-image diffusion models with reward backpropagation. 2023. 3
- [30] Alec Radford, Jong Wook Kim, Chris Hallacy, Aditya Ramesh, Gabriel Goh, Sandhini Agarwal, Girish Sastry, Amanda Askell, Pamela Mishkin, Jack Clark, et al. Learning transferable visual models from natural language supervision. In *International conference on machine learning*, pages 8748–8763. PmLR, 2021. 3, 6
- [31] Rafael Rafailov, Archit Sharma, Eric Mitchell, Christopher D Manning, Stefano Ermon, and Chelsea Finn. Direct preference optimization: Your language model is secretly a reward model. *Advances in Neural Information Processing Systems*, 36:53728–53741, 2023. 1, 3, 4
- [32] Robin Rombach, Andreas Blattmann, Dominik Lorenz, Patrick Esser, and Björn Ommer. High-resolution image synthesis with latent diffusion models. In *Proceedings of the IEEE/CVF conference on computer vision and pattern recognition*, pages 10684–10695, 2022. 1, 2, 3, 6
- [33] Chitwan Saharia, William Chan, Saurabh Saxena, Lala Li, Jay Whang, Emily L Denton, Kamyar Ghasemipour, Raphael Gontijo Lopes, Burcu Karagol Ayan, Tim Salimans, et al. Photorealistic text-to-image diffusion models with deep language understanding. *Advances in Neural Information Processing Systems*, 35:36479–36494, 2022. 3
- [34] Christoph Schuhmann. Laion-aesthetics. <https://laion.ai/blog/laion-aesthetics/>, 2022. Accessed: 2023-11-10. 6
- [35] Noam Shazeer and Mitchell Stern. Adafactor: Adaptive learning rates with sublinear memory cost. In *International Conference on Machine Learning*, pages 4596–4604. PMLR, 2018. 6
- [36] Aaron Van Den Oord, Oriol Vinyals, et al. Neural discrete representation learning. *Advances in neural information processing systems*, 30, 2017. 3
- [37] Bram Wallace, Meihua Dang, Rafael Rafailov, Linqi Zhou, Aaron Lou, Senthil Purushwalkam, Stefano Ermon, Caiming Xiong, Shafiq Joty, and Nikhil Naik. Diffusion model alignment using direct preference optimization. In *Proceedings of the IEEE/CVF Conference on Computer Vision and Pattern Recognition*, pages 8228–8238, 2024. 1, 2, 3, 4, 5, 6, 7, 8
- [38] Xiaoshi Wu, Yiming Hao, Keqiang Sun, Yixiong Chen, Feng Zhu, Rui Zhao, and Hongsheng Li. Human preference score v2: A solid benchmark for evaluating human preferences of text-to-image synthesis. *arXiv preprint arXiv:2306.09341*, 2023. 3, 6, 8
- [39] Enze Xie, Junsong Chen, Junyu Chen, Han Cai, Haotian Tang, Yujun Lin, Zhekai Zhang, Muyang Li, Ligeng Zhu, Yao Lu, et al. Sana: Efficient high-resolution image synthesis with linear diffusion transformers. *arXiv preprint arXiv:2410.10629*, 2024. 1
- [40] Jiazheng Xu, Xiao Liu, Yuchen Wu, Yuxuan Tong, Qinkai Li, Ming Ding, Jie Tang, and Yuxiao Dong. Imagereward: Learning and evaluating human preferences for text-to-image generation. *Advances in Neural Information Processing Systems*, 36:15903–15935, 2023. 6
- [41] Kai Yang, Jian Tao, Jiafei Lyu, Chunjiang Ge, Jiabin Chen, Weihang Shen, Xiaolong Zhu, and Xiu Li. Using human feedback to fine-tune diffusion models without any reward model. In *Proceedings of the IEEE/CVF Conference on Computer Vision and Pattern Recognition*, pages 8941–8951, 2024. 3
- [42] Jiahui Yu, Yuanzhong Xu, Jing Yu Koh, Thang Luong, Gunjan Baid, Zirui Wang, Vijay Vasudevan, Alexander Ku, Yinfei Yang, Burcu Karagol Ayan, et al. Scaling autoregressive models for content-rich text-to-image generation. *arXiv preprint arXiv:2206.10789*, 2(3):5, 2022. 6, 8
- [43] Huizhuo Yuan, Zixiang Chen, Kaixuan Ji, and Quanquan Gu. Self-play fine-tuning of diffusion models for text-to-image generation. *Advances in Neural Information Processing Systems*, 37:73366–73398, 2025. 3
- [44] Huaisheng Zhu, Teng Xiao, and Vasant G Honavar. Dspo: Direct score preference optimization for diffusion model alignment. In *The Thirteenth International Conference on Learning Representations*. 3, 4

Appendix for SUDO: Enhancing Text-to-Image Diffusion Models with Self-Supervised Direct Preference Optimization

a black angry cat with headphones on being a dj on a techno festival, with roaring animals as a crowd. hyping them up as they dance and rave



a photo of a woman



a 8x12m room, with walls, no ceiling, view from corner, grey pattern tiled floor, clear blue sky, sun not showing, one of the walls have several species of plants in vases



Jessica from rick and morty



dreadful environment art



ingeniero civil



SD1.5

DPO

SFT

SUDO

Figure 1. Extra qualitative comparisons with the SD1.5 base model.

The gate to the eternal kingdom of angels, fantasy, digital painting, HD, detailed.



Warsaw cyberpunk style at night



A group of elephants in camo gear sitting in a speeding jeep and hunting poachers



Детский сад аква



A 3d rendered emoji of a monster



cyberpunk robot



SDXL

DPO

SFT

SUDO

Figure 2. Extra qualitative comparisons with the SDXL base model.